# 18B.4 SUB-KILOMETER NUMERICAL PREDICTIONS IN THE NOCTURNAL STABLE BOUNDARY LAYER

David R. Stauffer[1]*, Brian J. Gaudet[1], Nelson L. Seaman[1], John C. Wyngaard[1], Larry Mahrt[2] and Scott Richardson[1]

[1]Pennsylvania State University, University Park, Pennsylvania
and
[2]COAS, Oregon State University, Corvallis, Oregon

## 1. INTRODUCTION

Meteorological models often are significant contributors to errors in atmospheric transport and dispersion (AT&D) predictions. Wind errors can be especially large in the nocturnal stable boundary layer (SBL). When synoptic forcing is weak, erratic near-surface sub-mesoscale flows can even lead to measurable transport upwind from the mean direction (Mahrt et al. 2008). Because turbulence tends to be so weak in the shallow nocturnal SBL, compared to deep convective boundary layers, these cases are much more likely to exhibit poor dispersion characteristics, thus maintaining high concentrations of airborne contaminants for many hours.

In stable conditions, the buoyancy production term of the turbulent kinetic energy (TKE) equation acts to suppress vertical motion, so SBL wind fluctuations are limited mostly to the horizontal. If the mean transport is light (~2 $ms^{-1}$ or less), the fluctuations are of the same order as the mean speed. This results in *SBL meandering*, defined here as horizontal transport in directions significantly different from the mean caused by large gentle or sudden shifts of SBL wind direction unrelated to local turbulence (Mahrt 2008). While occasionally exhibiting fairly regular behavior, meandering is more likely to be erratic and non-periodic. Dataset analysis suggests that such wind fluctuations in the SBL are dominated by features in the mesogamma (2-20 km) and sub-meso (20-2000 m) scales (Mahrt 2009a). Analysis of datasets led Hanna (1983) to conclude the two most probable factors contributing to SBL plume meandering are near-surface density-driven currents over irregular terrain and transient internal gravity waves aloft. However, Mahrt (2008) discusses numerous additional processes, so the physics responsible for shallow sub-meso and mesogamma-scale wind fluctuations in the SBL remains poorly understood.

In this study we continue recent DTRA-sponsored numerical research at Penn State University (PSU) investigating SBL predictability at very fine mesoscale resolutions. To meet this objective, model evaluations focus on the sub-meso and mesogamma scales, neither of which is resolved by the standard synoptic meteorological observing network. Thus, model evaluation must span all scales from the synoptic scale to the plume scale. This is an ambitious effort requiring advanced numerical modeling tools and specially designed local observations to augment the standard meteorological database.

We hypothesize that an NWP model configured with sub-kilometer resolution, higher-order numerics and minimal diffusion may facilitate simulation of at least the statistics of mesogamma-scale wind variance in the SBL. In this study a nested-grid model is used to simulate real cases of weakly forced flows in the nocturnal SBL over central PA, including sub-meso and mesogamma scale wind fluctuations on time scales of 20-120 minutes. Case studies and multi-case compositing are used to investigate the model's predictive characteristics for the mean and fluctuating wind components in the SBL.

## 2. NUMERICAL MODEL AND EXPERIMENT DESIGN

The model chosen for this research is the Weather Research and Forecasting (WRF) system's Advanced Research WRF (ARW) version 2.2.1 (Skamarock et al. 2005). To study the evolution of SBL flows, ARW is configured with four nested domains, each having a one-way interface with the next smaller grid. Table 1 gives the grid resolutions, time steps and number of horizontal points in each domain, while Fig. 1 shows domain locations. The finest domain covers ~67 km X 67 km, has a horizontal resolution of 444 m and is centered over the Nittany Valley of central PA (Fig. 2). This region is dominated by narrow quasi-parallel ridges flanking broad valleys oriented southwest-to-northeast with the Allegheny Mountains located in the northwest part of the domain. The 1.333-km domain covers ~160 km X 160 km, encompassing almost the entire Allegheny Mt. region (not shown), but it resolves the narrow ridge-and-valley topography of Central PA with lesser fidelity.

| Domain No. | Horiz. Res. (km) | Time Step (s) | No. of Points |
|---|---|---|---|
| 1 | 12.000 | 30 | 421 X 271 |
| 2 | 4.000 | 15 | 193 X 169 |
| 3 | 1.333 | 5 | 121 X 121 |
| 4 | 0.444 | 2.5 | 151 X 151 |

*Table 1. Resolution, time step and size of nested-grid WRF domains. All domains have 43 layers in vertical.*

* *Corresponding author address*: David R. Stauffer, Penn State Univ., Dept. of Meteorology, University Park, PA 16802; e-mail: stauffer@meteo.psu.edu

The model experiments are designed with two different vertical configurations. In the first, all four domains have 43 layers, with 11 layers in the lowest 68 m above ground level (AGL) (Fig. 3a). The lowest 5 layers in this high-resolution configuration have thicknesses of 2 m each, after which the layer depths gradually increase with height up to the model top at 50 hPa. The very fine vertical resolution near the surface is designed to resolve SBL structure and its dominant physical processes. In the second configuration, the region below 68 m AGL is consolidated into just two layers (Fig. 3b), representing more conventional layer thicknesses near the surface similar to those currently found in typical operational mesoscale models. The total number of layers in this standard vertical resolution configuration is 34. Since both configurations have the same nested horizontal domains, we can conveniently examine four solutions that reveal the sensitivity of model predictions to very high horizontal and vertical resolution (Table 2). The 0.444-km solution using the high-vertical resolution of Fig. 3a will be our *Baseline Experiment.*

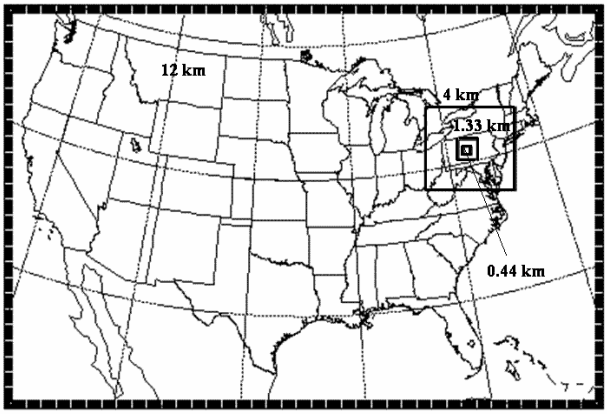


*Figure 1. Four-domain nested grid configuration of WRF.*

We note that the Baseline model configuration is designed specifically for investigating stable conditions. Thus, the sub-kilometer WRF forecasts are run daily for 12 h during the nocturnal period, beginning at 0000 UTC. With a time step on the innermost domain of 2.5 s, the 12-h forecasts are completed in ~ 6 h using four nodes of a Linux cluster at PSU, each node having four 3-GHz CPUs. Output files on the entire 1.333- and 0.444-km domains are saved at 12-minute intervals and over the local observing network at 10-s intervals to support analysis of sub-meso and mesogamma-scale fluctuations in the model. All experiments are run with the Mellor-Yamada-Janjic (MYJ) turbulence scheme (Janjic 2002), the Dudhia shortwave/ RRTM longwave radiation schemes, simple ice microphysics and thermal diffusion five-layer soil model (Skamarock et al. 2005).

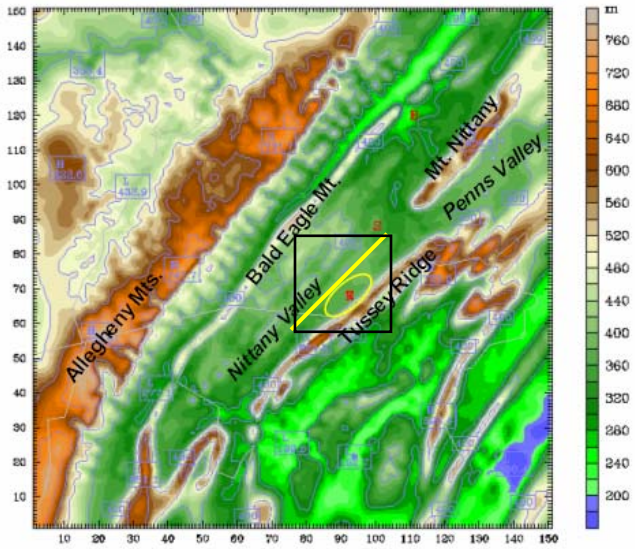


*Figure 2. Topography of WRF on Domain 4, horizontal resolution 444 m. The R indicates the location of Rock Springs within the oval denoting the site of the local obs network, and the region inside of the small square represents the subdomain shown in Fig. 11.*

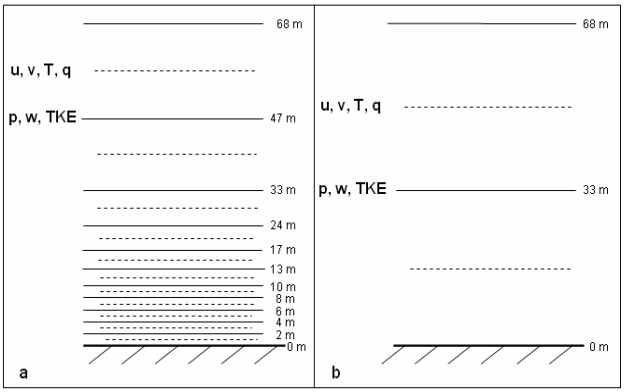


*Figure 3. WRF vertical configurations below 68 m AGL. Baseline configuration shown in (a); conventional vertical-resolution configuration shown in (b).*

| Exper. Name | Horiz. Grid (km) | Sfc. Layer Depth (m) | Layers Below 68 m |
|---|---|---|---|
| Baseline | 0.444 | 2 | 11 |
| LrgDZ | 0.444 | 30 | 2 |
| LrgDX | 1.333 | 2 | 11 |
| LrgDXDZ | 1.333 | 30 | 2 |

*Table 2. Design for the Baseline Experiment. and three additional sensitivity experiments.*

## 3. CENTRAL PA OBSERVING NETWORK

The sub-kilometer model grid described in Section 2 is needed to fully resolve fine-scale terrain features in

the Nittany Valley (Fig. 2) expected to dominate near-surface drainage winds, internal gravity-wave propagation and the vertical structure of the SBL. To evaluate the model's predictions at this scale, it is critical to obtain local wind and temperature data in the valley. Thus, a network of instrumented towers was deployed in a gently rolling terrain section of Nittany Valley near Rock Springs, close to the northwest base of Tussey Ridge (yellow ellipse, Fig. 2). This valley site is ideal for our purpose because the quasi-linear ridge-and-valley topography of central PA makes it easier to separate the role of regional versus local terrain forcing. Also, the rolling topography of Nittany Valley is typical of the terrain over much of the Eastern U.S.

Wind speed and direction at Rock Springs are measured using Vaisala WS425 two-dimensional (2-D) sonic anemometers. These instruments have a very low starting threshold (~0.10 $ms^{-1}$) and 1 Hz sampling rate. In late summer 2007 the first five 2-D sonic anemometers were deployed in a preliminary "scoping" network on 10-m towers at elevations of 3 and 10 m AGL, along with 10 Campbell thermistors to measure temperature. The raw data are collected in real time and averaged to one-minute intervals for quality checking, distribution and archival. Seven additional 2-D and 3-D sonics and five more thermistors were deployed in early 2008. Three of the new sonics and thermistors were deployed on a 50-m tower.

## 4. MODEL RESULTS AND EVALUATION

### 4.1 *Evaluation on Coarse Domains*

Before evaluating local solutions for the SBL on the model's inner domains in PA, WRF's accuracy for predicting the synoptic and mesoalpha scales must be established. Meso-alpha-scale domain-wide statistical evaluation was performed using the Model Evaluation Toolkit (MET) code provided by the WRF Development Testbed Center (DTC) in Boulder, CO. We have modified MET to include wind direction statistics, and scripted MET to run nightly following each model forecast cycle to validate the forecasts on the two outer domains against standard surface METAR and radiosonde data. Here we present root mean square errors (RMSE) and bias errors for wind speed, wind direction, and temperature versus pressure for the sixteen-case composited 12-h ARW predictions (1200 UTC) on the 12-km and 4-km domains (Figs. 4-6). We find that wind speed bias errors are generally less than 1 $ms^{-1}$ but become positive near the surface; RMSE scores are lowest in the mid-troposphere for wind speed, and lowest in the upper troposphere for wind direction. Temperature RMSE scores are generally less than 1.5 C except in the lowest 750 m, where a substantial cold bias exists. We note these errors generally are comparable to other recently reported season-averaged forecast errors for similar domains (Koch and Gall 2005; Nance et al. 2007).

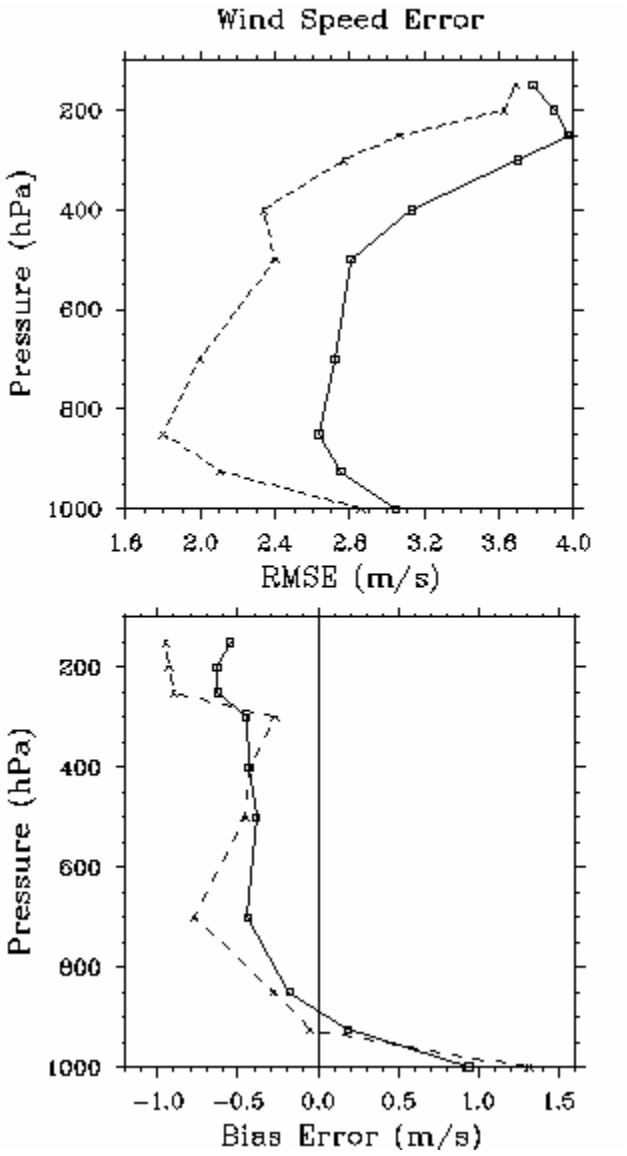


*Figure 4. Sixteen-case composite RMSEs (top) and bias errors (bottom) for wind speed in 12-h WRF forecasts for autumn 2007 on 12-km domain (solid) and 4-km domain (dashed).*

### 4.2 *Evaluation on Local Domains*

For the final step of this preliminary model evaluation, winds predicted by WRF at Rock Springs, PA, (R in Fig. 2) are verified against data from the local field network. Since plume transport and dispersion is the cumulative result of integrated mean wind and turbulence acting on air parcels, it is important to examine the high-frequency fluctuating component of the predicted low-level state variables in addition to their lower-frequency mesoscale behavior.

We begin by comparing the observed and model-predicted wind speed and direction for a typical case at Tower Site 1 (Figs. 7 and 8). This site is located ~ 0.75 km from the base of Tussey Ridge (~2.5 km southwest of "R" in Fig. 2). Figure 7 shows 12-h time series of one-minute averaged observed and predicted speeds at 3 m and 10 m AGL for the night of 7 October 2007. Both of the time series contain a range of frequencies, but all the fluctuations are too low-frequency to be associated with the weak turbulence in the SBL. To isolate the more-predictable low-frequency com-ponent, Gaudet (2008) applied a 2-h running mean filter to the model's time series, yielding the smoother curve shown here in red. Figure 7 shows the dominant non-turbulent fluctuations in the model of ~0.3-2.0 h resemble the observations, while higher-frequency variability is poorly captured by WRF. We hypothesize that these large lower-frequency fluctuations are associated primarily with the passage of mid-level internal gravity waves propagating through the model atmosphere and modulating the near-surface drainage winds.

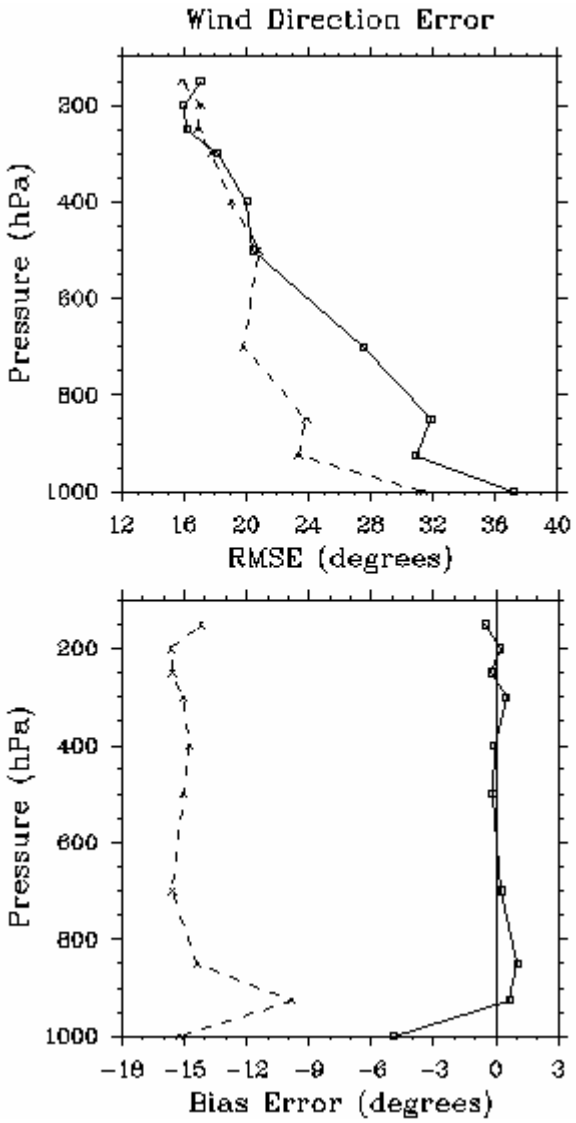


*Figure 5. Same as Fig. 4, but for composite RMSEs (top) and bias errors (bottom) for wind direction.*

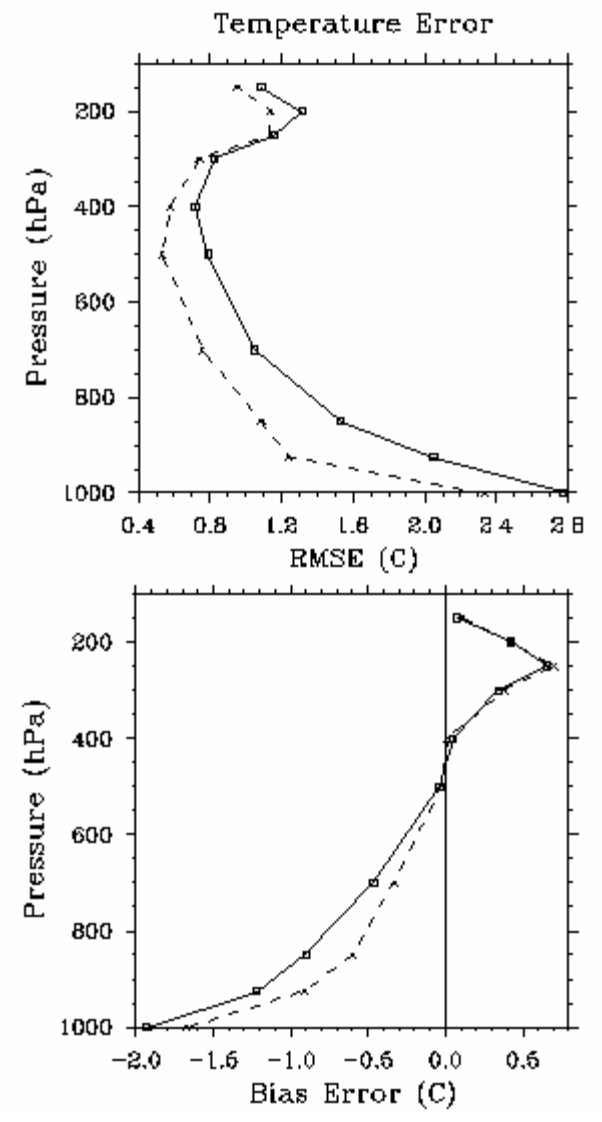


*Figure 6. Same as Fig. 4, but for composite RMSEs (top) and bias errors (bottom) for temperature.*

Figure 8 shows a similar comparison of 12-minute averaged nocturnal wind directions observed and forecasted for the 7 October case at Site 1 near the base of Tussey Ridge. The observed winds have a mean direction of ~210 degrees through most of the night, with large fluctuations of about +/- 100 degrees. However, WRF predicted a mean nocturnal wind direction of ~250 degrees, representing an error in mean direction of ~40 degrees at this site. Visual inspection of model-predicted horizontal flow near Rock Springs (not shown) indicates the local winds turn sharply over a distance of 1-2 km in the vicinity of this site due to the influence of a nearby row of low hills. Even though the model has captured the dominant direction (southwest) in the Nittany Valley, local distortion of the winds close to these hills leads to large direction errors at this site. Meanwhile, Figure 8 shows that direction fluctuations in WRF for this night also are about +/-100 degrees, on the same scale as those observed, but only during periodic bursts. We note that very few previous numerical investigations have been able to generate fluctuations of predicted speed and direction on time scales shorter than an hour in a manner having any apparent relationship to observations. We believe these non-turbulent mesogamma-scale fluctuations are critical to understanding and predicting realistic plume behavior in stable light-wind conditions, including plume meandering.

The importance of enhanced horizontal and vertical model resolution to these predictions can be seen in Fig. 9, comparing filtered wind speed output for the different sensitivity experiments described in Table 2. It can be seen that the combination of high vertical and horizontal resolution are required for the best prediction of the observations, but the sensitivity is somewhat higher to the increased horizontal resolution. Even with the highest resolution experiment, however, a positive wind speed bias remains. Keep in mind that even the coarser horizontal grid spacing is 1.333 km, and the wind speeds shown in the figure are generally less than 2 $ms^{-1}$.

Based on the evaluations shown in Figs. 7 and 8, a running-mean temporal filter was applied to all cases having strong nocturnal SBLs during Oct-Nov 2007. This procedure separated the low-frequency deterministic component of the model solutions from the higher-frequency components found to be mostly non-deterministic in terms of their poor correlation with observed fluctuations of the same scale (Gaudet 2008). By compositing these filtered time series over the 16 autumn cases found to have well-developed nocturnal SBLs, it is apparent that WRF predicts the very weak wind speeds at 9 m AGL quite well on the 0.444-km domain, but the 1.333-km grid has a much larger positive speed bias (Fig. 10). It is hypothesized that the model's failure to simulate gradually decreasing speeds through the night may be due to certain characteristics of the MYJ PBL scheme.

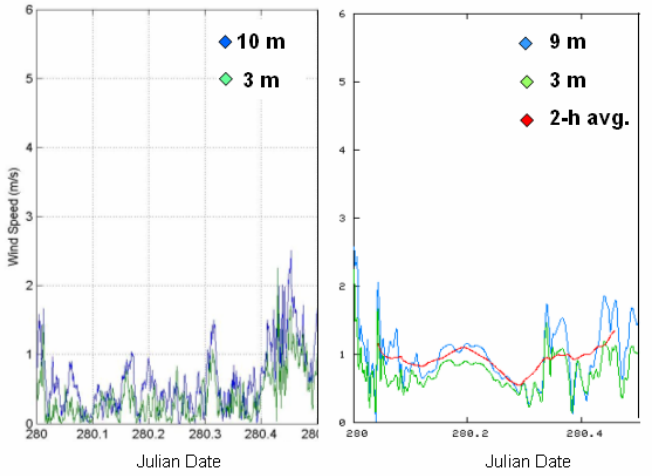


*Figure 7. Comparison of observed (left) and forecasted (right) wind speeds ($ms^{-1}$) at Site 1, Rock Springs, PA, for the period 0000-1200 UTC, 7 October 2007. Red shows 2-h running mean for model prediction, based on average of 3-m and 10-m winds.*

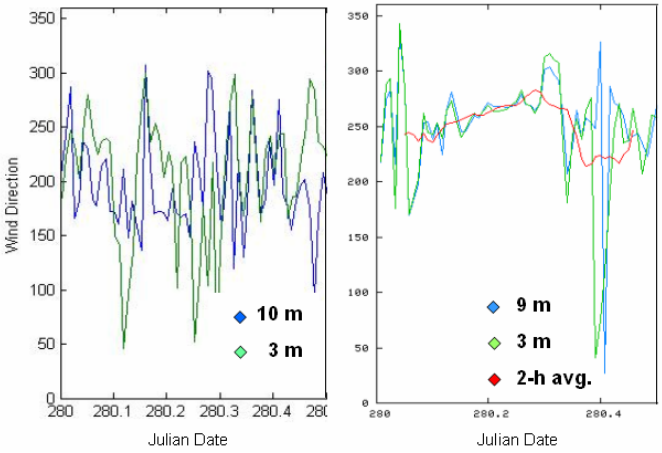


*Figure 8. Same as Fig. 7, but for observed (left) and forecasted (right) wind directions (deg).*

Although the higher-frequency fluctuations removed from the model-predicted time series have low correlation coefficients when compared to the observed fluctuations (not shown), they are found to have similar spectra for time scales of ~20-120 minutes (Gaudet et al. 2008). At these time scales, they can contribute significantly to stable plume meandering in the SBL. Insight into the impact these high-frequency wind fluctuations may have on transport in the SBL can be appreciated by examining parcel trajectories for some individual cases.

Figure 11 presents 3-h trajectories for nine parcels released near Rock Springs, PA, from a height of 3 m AGL at 0800 UTC, 7 Oct 2008. At the initial time the parcels span the horizontal area of one grid cell on Domain 4 (i.e., 444 m X 444 m square). The top panels of Fig. 11 show trajectories computed on Domain 4 (444-m horizontal grid spacing) using model velocities output every 12 minutes (top left) and every 1 h (top

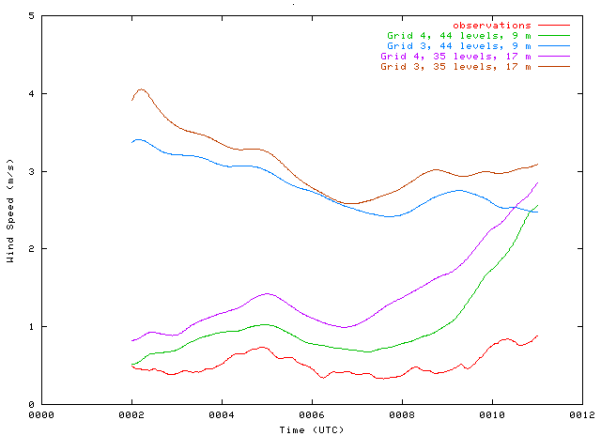


*Figure 9. Comparison of observed and modeled filtered wind speeds ($ms^{-1}$) at Site 1, Rock Springs, PA, for the period 0000-1200 UTC, 7 October 2007. The lowest speed curve represents the observations (red) followed by the model experiments as described in Table 2 in order of increasing speed: Baseline experiment (green), LrgDZ (magenta), LrgDX (blue), and LrgDXDZ (brown).*

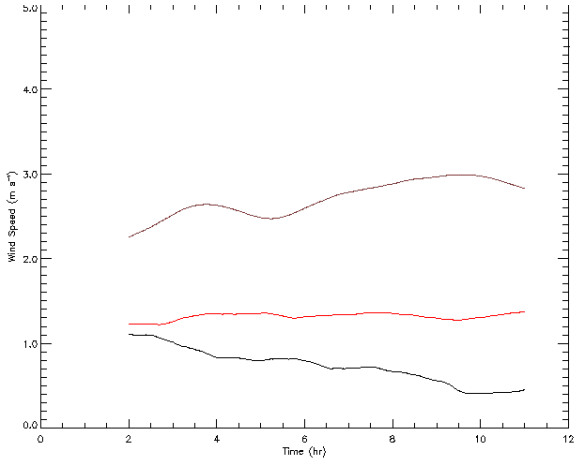


*Figure 10. Filtered deterministic component of speed ($ms^{-1}$) in nocturnal SBL at 9 m AGL, composited over 16 autumn cases. Shown are observed speed (black) versus model speed on 0.444-km domain (red)) and 1.33-km domain (purple).*

right). Without sub-grid dispersion the cluster of parcels moves toward the northeast carried by the mean southwesterly winds (~1 $ms^{-1}$) in the SBL. This direction is consistent with the most frequent directions observed in the valley. However, due to the periodic fluctuations in wind direction, many of the parcels in Fig. 11a move in a sinusoidal manner characteristic of a classic meandering plume. The trajectories from 1-h velocity data in Fig. 11b migrate in the same general direction in the valley, but with less structure and inter-parcel variability. After ~3 h, about half of the parcels in Fig. 11b are suddenly advected over Tussey Ridge, while parcels with the 12-minute velocity data in Fig. 11a are still in the valley.

Figures 11c and 11d show trajectories released from the same 444 m x 444 m area, but within Domain 3 (1.333-km horizontal grid spacing) using 12-minute and 1-h model wind data, respectively. The importance of having horizontal grid spacing less than even 1 km for some cases is clearly shown: all parcels are advected uniformly and rapidly over Tussey Ridge within Domain 3, compared to all or many parcels staying in the valley within Domain 4 in Figs. 11a and 11b.

For this example, finer horizontal resolution is very important for predicting the weak SBL wind speeds (Fig. 9), and finer temporal resolution using 12-minute versus 1-h velocity updates further improves the ability of the model to produce SBL meandering flows (Fig. 11).

As expected from real cases, model-computed trajectories vary from night to night. On other nights (not shown), parcel trajectories sometimes form nearly circular looping patterns for several hours, or parcels may reverse direction as they respond to large shifts of the near-surface ABL wind direction. This may occur when channeled winds in Nittany Valley interact with mesoscale features farther aloft. The statistical behavior of these fluctuations can be explored in the form of spectra based on the predicted and observed wind time series (Gaudet et al. 2008).

## 5. SUMMARY

In this study, an instrumented field network and a specially configured version of WRF-ARW have been used to investigate predictability of SBL structure and behavior based on horizontal, vertical and temporal model data resolution. Using very fine temporal and horizontal grid resolution and the MYJ PBL scheme, it has been shown that the modeling system can predict important aspects of the nocturnal SBL, such as the wind speed and direction fluctuations associated with stable plume meandering. The coarser vertical resolution experiments produce lowest model-level wind output at 17 m AGL, and thus the wind speeds are predicted to be stronger than the high vertical resolution experiments. Local field measurements in central PA indicate strong vertical gradients in wind speed within the lowest 10 m AGL (not shown). Thus without sufficient horizontal, vertical and temporal resolution atmospheric data, the qualitative and quantitative characterstics of SBL weak-flow trajectories can be very different.

Future analysis of field data from a 50-m tower will evaluate predictions of SBL vertical structure. PSU also is exploring options to acquire remote sensing instruments to observe internal gravity waves aloft. Additional work will extend the model evaluations to include testing of the Quasi-Normal Scale Elimination (QNSE) PBL scheme of Galperin et al. (2007).

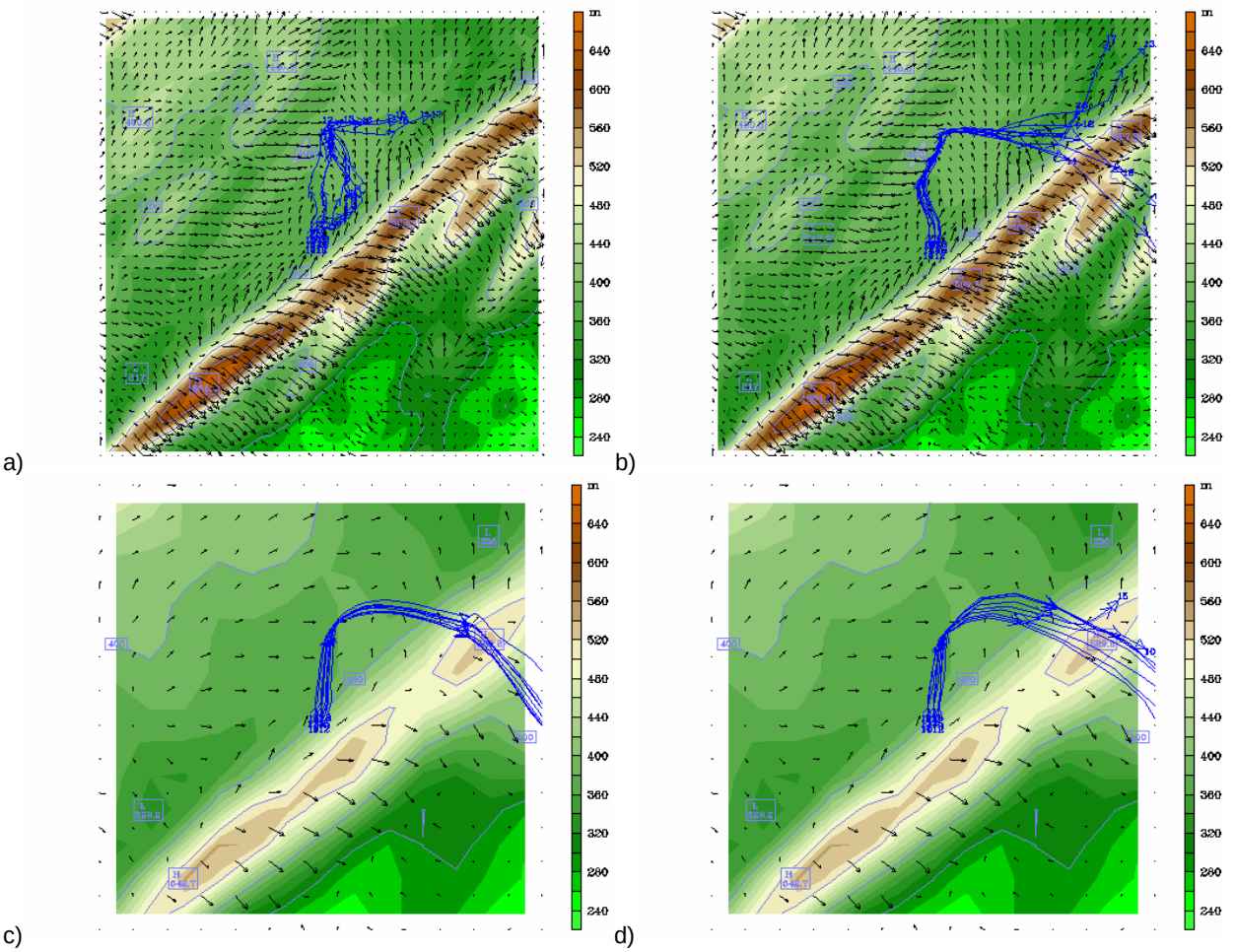


*Figure 11. Meandering trajectories in Nittany Valley (0800-1112 UTC) for nine parcels released near Rock Springs at 3 m AGL and predicted wind vectors at 1112 UTC, 7 Oct 2007, within WRF-ARW. a: Baseline 0.444-km domain with 12-minute updated model velocities; b: Baseline 0.444-km domain with 1-h updated model velocities; c: LrgDX 1.333-km domain with 12-minute updated model velocities; d: LrgDX 1.333-km domain with 1-h updated model velocities.*

*Acknowledgements*: This research has been sponsored by the Defense Threat Reduction Agency under contract no. W911NF-06-1-0439-MOD-P00001 under the supervision of Dr. John Hannan. We also acknowledge the Development Testbed Center in Boulder, CO, for providing assistance with its MET codes and Mr. Glenn Hunter and Mr. Jeffrey Zielonka of Penn State for assistance with a number of the figures.

## 6. REFERENCES

Galperin, B., S. Sukoriansky, and P.S. Anderson, 2007: On the critical Richardson number in stably stratified turbulence. *Atmos. Sci. Let.*, **8**, 65-67.

Gaudet, B.J., 2008: Definitions of determinism. 9th WRF Users' Workshop, Boulder, 23-27 June, 4 pp.

Gaudet, B.J., N.L. Seaman, D.R. Stauffer, S. Richardson, L. Mahrt, and J.C. Wyngaard, 2008: Verification of WRF-predicted mesogamma-scale spectra in the SBL using a high-frequency filter decomposition. 9th WRF Users' Workshop, Boulder, 23-27 June, 4 pp.

Hanna, S.R., 1983: Lateral turbulence intensity and plume meandering during stable conditions. *J. Clim. Appl. Meteor.*, **22**, 1424-1430.

Janjic, Z.I., 2002: Nonsingular implementation of the Mellor-Yamada Level 2.5 Scheme in the NCEP Meso model. NCEP Office Note 437, 61 pp. Available online at http://www.ncep.noaa.gov.

Koch, S.E. and R. Gall, 2005: The DTC Winter Forecast Experiment: Final Project Report. Available from Development Testbed Center, Boulder, CO, 27 pp.

Mahrt, L., 2008: Mesocale wind direction shifts in the stable boundary-layer. *Tellus*, **60A**, 700-705.

Mahrt, L., 2009a: Characteristics of submeso winds in the stable boundary layer. *Bound-Layer. Meteor*., **130**, 1-14.

Mahrt, L., D. Stauffer and N. Seaman, 2008: Analysis of observed wind variability in the stable boundary layer using meso-networks. *Chem. Bio. Def.: Phys. Sci. & Tech. Conf.*, New Orleans, LA, 17-21 November, 3 pp.

Nance, L., L.R. Bernardet, B. Weatherhead, G. Noonan, T. Fowler, T.G. Smirnova, S.G. Benjamin, J. Brown, and A. Loughe, 2007: Weather research and forecasting core tests. AMS 22nd Wea. Anal. Fcstng. Conf./18th Num. Wea. Pred. Conf., Park City, UT, 25-29 July.

Skamarock, W.C., J.B. Klemp, J. Dudhia, D.O. Gill, D.M. Barker, W. Wang and J.G. Powers, 2005: A description of the advanced research WRF version 2. NCAR Tech. Note NCAR/TN-468+STR, 88 pp.